The Endourological Society Summer Student Scholarship

Student: Alan Shain
Mentor(s): Dr. Shaun Wason, Dr. David Wang, Dr. Daniel Leslie, Dr. Sheila Russo.
Institution: Boston Medical Center (Boston University School of Medicine)

Title of Project: Prototyping and Testing a Novel Soft Robotic Anti-retropulsion Device for Ureteroscopy.

Background and Objective:

Retrograde migration of stone fragments (retropulsion) during ureteroscopic lithotripsy increases surgical time and reduces the stone-free rate.[1] Currently available, wire-based anti-retropulsion devices incompletely block the upper urinary tract, especially in dilated ureters. One prominent early balloon anti-retropulsion device - Passport™ - has the same limitations since it is manufactured from a non-compliant material (only expanding to 4 mm),[1] allowing stone fragments and irrigant fluid to bypass the device and migrate up the ureter. Other devices, such as the Percsys Coax Accordion™ device and BackStop™ Gel, were more successful in ureteral occlusion at larger diameters,[1] however are no longer in production. Literature has shown that the vast majority of proximal and distal ureteral calculi (greater than 95%) were associated with ureteral dilation of 10 mm or less.[4] An effective anti-retropulsion device should be able to prevent retropulsion for the vast majority of stones in a wide variety of ureteral diameters. Using computer modeling software, ABAQUS, we designed an anti-retropulsion device 1 mm thick and planar, resulting in deformations greater than 12mm at 10kPa (1.5 PSI), large enough to prevent stone migration in a dilated ureter.[2] In theory, the prototype should conform to the irregular geometry of the ureter upon deployment with low-pressure actuation to minimize potential tissue trauma when compared with the high pressure, low compliance Passport™ balloon (861 kPa, 125 PSI), or metal devices.[5] The final design should be easy to manufacture, occlude the entire diameter of the ureter, and actuate with low pressure to minimize stress on the ureter.[2] The objective of our study was to fabricate and test our soft-robotic anti-retropulsion prototype using an *in-vitro* ureteroscopy model.

Methods:

Prototype devices were fabricated by casting a highly compliant, platinum-catalyzed silicone polymer (Ecoflex™ 00-30) in a 3-D printed mold at the Materials Robotics Laboratory at Boston University. Our prototype dimensions were 1 mm (height) x 5 mm (width) x 15 mm (length). The compliance and cross sectional area for 3 separate prototype devices were measured in triplicate (n=9). Device dimensions were measured in two orthogonal orientations. The device dimensions under pressure actuation (width and height) are currently undergoing image analysis processing using adobe illustrator to measure cross-sectional area for each corresponding volume.

The performance of the anti-retropulsion device was compared with control (no device) and two other anti-retropulsion devices - StoneCone™ (Boston Scientific, Boston, MA) and Percsys Coax Accordion™ (Percutaneous Systems, Inc., Palo Alto, CA) - in an *in-vitro* ureteral model. The previously validated *in-vitro* ureteral model was designed by submerging clear acrylic tubing (9.53 mm (⅜ inch) inner diameter, 12.7 mm (½ inch) outer diameter) in normal saline (0.9 %) adjacent to a metric ruler.[3] Phantom stones (cylindrical, radius = 2.5 mm, height = 5 mm) were fabricated from Plaster-of-Paris, given its similar mechanical properties to kidney stones and prior use in an *in-vitro* model of retropulsion.[3] Phantom stones were subsequently fragmented with an electrohydraulic lithotripsy (EHL)

probe via a flexible ureteroscope (Dual lumen flexible ureteroscope, Richard Wolf, Vernon Hills, IL). Each test consisted of an EHL probe on low power (Autolith™ Touch, Boston Scientific, Boston, MA) using 100 pulses. 10 trials were performed for each experimental condition (one trial for StoneCone group retropulsion was unclear and excluded from analysis (n=9)).

With every pulse from the EHL probe, the phantom stone would migrate backwards and fragment. A fragment was defined as any part of the stone with weight > 0.001 grams and which was able to be extracted without disintegrating into dust upon extraction from the tube. In every trial, phantom stones started at the same position and broke into fragments, usually with a larger main fragment. Retropulsion was measured by recording the travel distance of the largest fragment after 100 EHL pulses. The retropulsion of the largest fragment ("retropulsion") and the number of fragments ("fragmentation") in each trial were recorded. The weight of each stone was recorded for the stone at the start of the trial and the combined weight of all fragments after the trial. The difference between pre- and post- lithotripsy weights was displayed as a percentage ("% weight loss"). The additional weight of saline was taken into account by dipping the phantom stones in saline and allowing 2 minutes to dry before recording pre-lithotripsy weight. Fragments post-lithotripsy were removed from the saline and also allowed 2 minutes to dry before recording their combined weight. For the experimental conditions, migration of the anti-retropulsion device in any direction was also recorded ("device migration"). Student's t-test was used to compare the mean of recorded variables (retropulsion, % weight loss, fragmentation, device migration) between the control group and each experimental group, and between each experimental group to each other.

Results:

The prototype design was modified from the computer model by asymmetrically adding 0.01 mm to the height, such that the thinner side actuated slightly more than the thicker side to produce a bend (Figure 1). This improved the prototype's occlusion properties in the *in-vitro* model. Compliance data demonstrates low average gauge pressure, 0.81 (+/- 0.05) PSI (Figure 2) at actuation volumes of 2.5 mL (maximum volume tested). Preliminary image analysis on one prototype (out of three total) revealed deformation beyond the cross-sectional area required to completely occlude a tube of 9.53 mm diameter when actuated at or above 1.25 mL (Figure 3).

Our prototype, Accordion™ and StoneCone™ all showed a statistically significant reduction in average stone retropulsion compared with the control in our *in vitro* model: our prototype vs control (2.8 +/- 0.3 cm vs 17.8 +/- 3.1 cm; $P < 0.05$; Table 2), Accordion™ vs control (3.0 +/- 0.4 cm vs 17.8 +/- 3.1 cm; $P < 0.05$; Table 2), StoneCone™ vs control (3.0 +/- 0.7 cm vs 17.8 +/- 3.1 cm; $P < 0.05$; Table 2). Importantly, the prototype did not let any stone fragments pass the device, since the balloon conformed to the diameter of the ureter; however Accordion™ allowed 1 fragment to lodge midway through its plastic folds in its deployed form and the StoneCone™ allowed multiple fragments to pass since it is purposefully designed with concentric rings that allow small fragment retropulsion. The prototype also exhibited the least device migration; however, the difference in average migration between devices was not statistically significant: the prototype vs StoneCone™ (0.2 +/- 0.63 cm vs 0.4 +/- 0.70 cm; $P > 0.05$; Table 2) and the prototype vs Accordion™ (0.2 +/- 0.63 cm vs 1.5 +/- 2.6 cm; $P > 0.05$; Table 2).

StoneCone™ had the highest % weight loss (Table 1) overall, which was statistically significant compared with the prototype (58.9% +/- 37.6 vs 18.8% +/-27.9; $P < 0.05$; Table 1). Accordion™ had the

highest stone fragmentation overall, which was statistically significant compared with the prototype (6 +/- 4 stones vs 2 +/- 1 stones; $P < 0.05$; Table 3).

Conclusion:

We successfully fabricated and tested our design for a novel soft-robotic anti-retropulsion prototype in a validated *in-vitro* retropulsion model. The prototype that was developed using highly compliant Ecoflex™ 00-30 material occluded the entire volume of the ureter model to prevent retropulsion under low pressure actuation. This low pressure actuation should prevent damage to the ureteral walls. The prototype performed similarly to other anti-retropulsion devices on the market, which all prevented retropulsion of the largest stone fragment significantly better than the control. The prototype also maintained a stable position in the *in-vitro* model due to its low average migration distance. With further analysis, the prototype could improve in stone fragmentation and % weight loss of the stone. We plan to focus on a delivery mechanism into the urinary system, potentially attaching our prototype to a guidewire, which could then be threaded through a dual lumen flexible ureteroscope.

Citations

1) Elashry, O. M., & Tawfik, A. M. (2012). Preventing stone retropulsion during intracorporeal Lithotripsy. Nature Reviews Urology, 9(12), 691–698. https://doi.org/10.1038/nrurol.2012.204

2) Leslie, D. C., Wang, L.B., McCandless, M., Lee, H., Russo, S., Wang, D.S., and Wason, S.W. (2021) "Computer Modeling for Optimization of Endourological Robotic Devices" *Oral presentation* at the New England American Urological Association Annual Meeting. Burlington, VT; October 14-16 2021.

3) Eisner, B. H., Pengune, W., & Stoller, M. L. (2009). Use of an antiretropulsion device to prevent stone retropulsion significantly increases the efficiency of pneumatic lithotripsy: An *in vitro* study. BJU International, 104(6), 858–861. https://doi.org/10.1111/j.1464-410x.2009.08540.x

4)Eisner, Brian H., et al. "Differences in Stone Size and Ureteral Dilation between Obstructing Proximal and Distal Ureteral Calculi." *Urology*, vol. 72, no. 3, 2008, pp. 517–520., https://doi.org/10.1016/j.urology.2008.03.034.

5) "Passport™ Balloon." *www.bostonscientific.com*, https://www.bostonscientific.com/en-EU/products/dilatation/passport.html.

Tables and Figures

TABLE 1. *Results of EHL comparing the weight change of a phantom stone before and phantom stone fragments after lithotripsy in the in-vitro model.*

	Experimental Conditions			
	Control (no device)	Accordion	StoneCone	Prototype
Weight (g) before EHL lithotripsy mean ($\pm$ std)	0.160 ($\pm$ 0.008)	0.158 ($\pm$ 0.008)	0.146 ($\pm$ 0.009)	0.161 ($\pm$ 0.009)
Weight (g) after EHL lithotripsy mean ($\pm$ std)	0.129 ($\pm$0.043)	0.100 ($\pm$ 0.044)	0.060 ($\pm$ 0.055)	0.131 ($\pm$ 0.046)
% weight loss mean ($\pm$ std)	18.9 ($\pm$ 25.0)	36.6 ($\pm$ 27.9)	58.9($\pm$ 37.6)	18.8 ($\pm$ 27.9)

TABLE 2. *Results of EHL comparing metrics evaluating retropulsion-prevention before and phantom stone fragments after lithotripsy in the in-vitro model.*

	Experimental Conditions			
	Control (no device)	Accordion	StoneCone	Prototype
Retropulsion of largest stone fragment (cm) mean ($\pm\ std$)	17.8 ($\pm$ 3.1)	3.0 ($\pm$ 0.4)	3.0 ($\pm$ 0.7)	2.8 ($\pm$ 0.3)
Migration of anti-retropulsion device (cm) mean ($\pm\ std$)	N/A	1.5 ($\pm$ 2.6)	0.4 ($\pm$ 0.70)	0.2 ($\pm$ 0.63)

TABLE 3. *Results of EHL comparing metrics evaluating the average number of fragments created from a phantom stone after lithotripsy in the in-vitro model.*

	Experimental Conditions			
	Control (no device)	Accordion	StoneCone	Prototype
Number of Stone fragments mean ($\pm$ std)	3 ($\pm$ 3)	6 ($\pm$ 4)	3 ($\pm$3)	2 ($\pm$ 1)

FIGURE 1. *Original prototype finite element model (top left) and original computer aided design prototype (bottom left) alongside final prototype (right).*

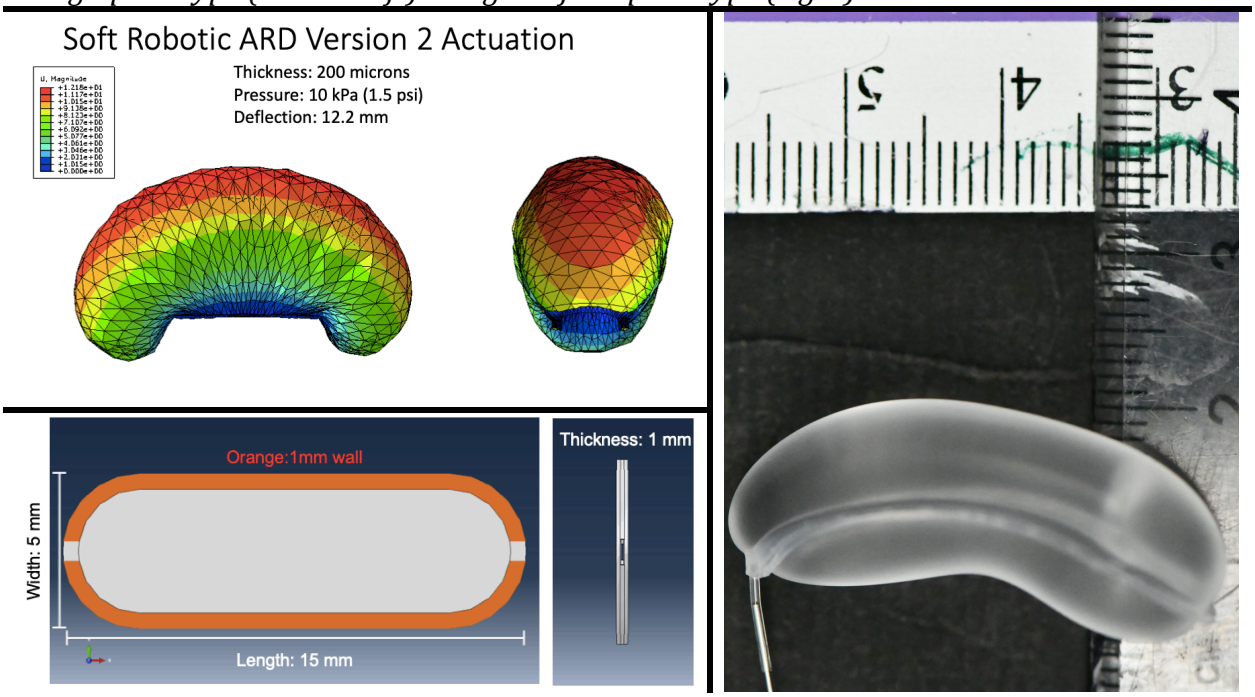

FIGURE 2. *Average measured pressure as function of infused saline volume in 3 prototype devices (n=3) each tested in triplicate (average +/- standard deviation).*

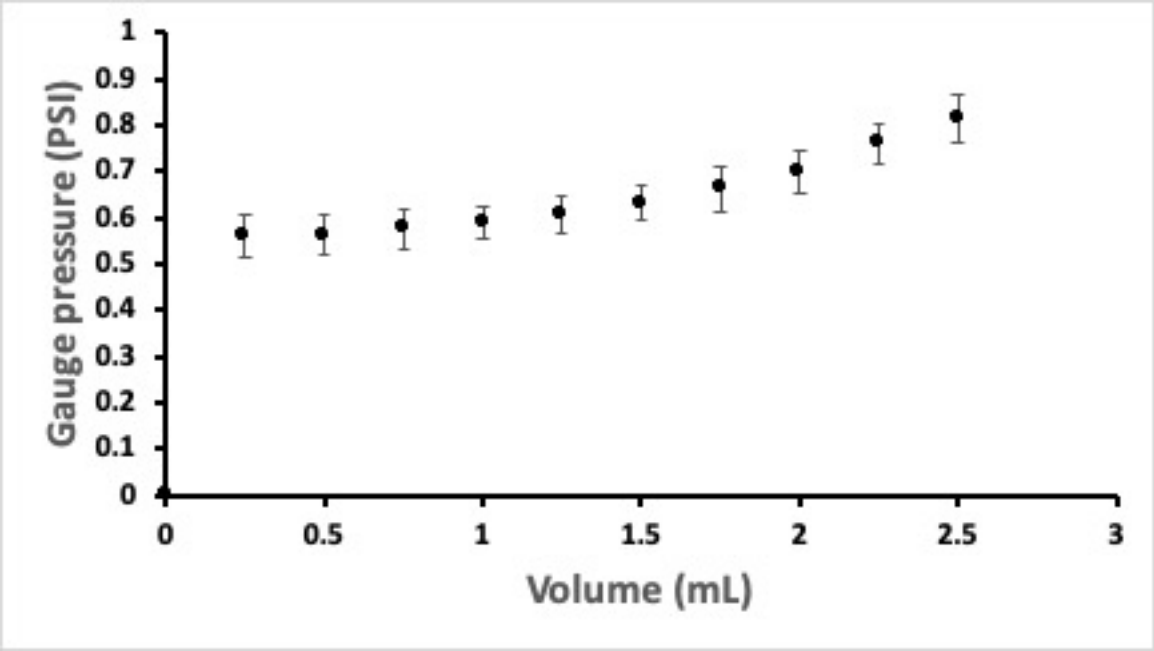

FIGURE 3. *Preliminary data on average cross-sectional area of 3 tests on 1 prototype as a function of infused saline volume into the device (average +/- standard deviation). Dashed line represents the cross-sectional area of the in-vitro tube model. Note: Data has yet to be analyzed on the other two prototypes test for this experiment and the method of analysis is still undergoing development.*